Investigation of Structural and Rheological properties of Metal nanoparticles

Shadab Khan, Sandhya Patel*[1], Prashant Shukla, Sameeksha Rajput,

Sanyam Jain, Priyanka Sahu

Abstract: Silver nanoparticles have been prepared by the addition of Ethylene Glycol and embedded into the matrix of PVA (Poly Vinyl Alcohol). Silver nanoparticles were compared with nanoparticles of ZnO, MnO, and Cu. Their structural properties are investigated using UV-Visible spectroscopy and Scanning electron microscopy (SEM). UV results showed that surface plasmon absorption is most prominent in Silver nanoparticles. Rheological studies of PVA-Silver nanoparticles composites where PVA acts as a stabilizer exhibited the non-Newtonian flow of these fluids.

Introduction

Noble metal nanoparticles have had a great impact on our day-to-day technology because of their tremendous applications. Metal nanoparticles, nanowires, nanotriangles, or nanosheets have a comparatively larger surface area rendering them very proficient in catalytic and percolating applications. Noble metal nanoparticles showcase immense sensitivity to the Localized surface plasmon resonance to the local dielectric of the surrounding environment. This sensitivity is responsible for superior refractive index sensing due to LSPR shift [1]. Out of these noble metal nanoparticles, the Silver nanoparticles have become the centre of attention of nanotechnologists because of their special optical, physical, and chemical properties. To test this theory we have compared the UV-Vis, FTIR, and SEM results of Silver nanoparticles with ZnO nanoparticles [2], MnO nanoparticles [3], and Cu nanoparticles [4].

Organic compounds have proven to be very useful in the field of optoelectronic and photonic devices. In the case, of solar cells, the growing demand is for more flexible devices which can be applied to different things, as energy harvested by solar cells is directly proportional to the surface area of the panel. As far as rheological properties are concerned high signal speed, high density, dependability, and low cost are some of the current trends in electronic packaging technology, which requires continuous advancement in related fields such as thick film ink formulation [5]. The two main technologies that have revolutionised the development of thick film paste are multilayer ceramic technology and microelectronic packaging which are used for formulations to obtain finer definition, line-width, etc. Depending on the co-firing temperature/atmosphere, a variety of thick film conductor pastes based on noble metals to base metals have been used for thick film-based multilayer ceramic processing [6]. Due to its excellent thermal conductivity, thermal expansion coefficient, electrical conductivity, and oxidation-reduction stability, silver-based polymer paste is the most recommended. The most important aspect of thick film paste is its rheology, which must be perfect to produce conducting interconnects with the necessary thickness, line width, and

[1]*Corresponding author mail: shadabanwar11@gmail.com, spatel@dhsgsu.edu.in

definition [7-8]. The performance of thick film paste is influenced by several factors, including percentage of solid loading, particle size, the characteristic temperature of permanent binders (Tg, Ts, melting temperature), morphology, viscosity, and rheological characteristics [9-10].

In our humble effort, we prepared AgNPs-PVA thin film paste that has unique characteristics tunable through their size and morphology. Ag-PVA nanocomposite pastes have been preferred because of their ease of preparation through chemical reduction. We present various Structural and Rheological studies of this film pastes. Cu, ZnO, Mn and Ag nanoparticles have been prepared using the economical and easy to accomplish Green synthesis. These structutal properties were analysed via Scanning Electron Microscopy (TEM), UV-Visible spectroscopy, and Fourier Transform Infrared spectroscopy (FTIR). In particular, we study Ag-PVA film paste for its rheological characteristics. We analyse the effect of Silver nanoparticles on the polymer that impacts the thixotropic behavior of nanocomposite.

Experimental details

The AgNPs solution was prepared using clove extract by adding 20ml of it to the 1.69g $AgNO_3$. Then PVA solution (made by mixing PVA polymer with the solvent of Deionised water) is added with AgNPs solution at 70% using a magnetic stirrer at 500rpm at 50^0C for 3 hours. Similarly, ZnO nanoparticles were prepared via green synthesis using Clove extract. In this process, 40ml of Zinc Acetate is added to the 20ml Clove extract at 50^0C for 20min. Cu nanoparticles are prepared by adding $Cu(NO_3)_2$ to the clove extract and adding NaOH as the reducing agent. In this method, 1.5g of $Cu(NO_3)_2$ is mixed with 20 ml of clove extract, and then 0.4g NaoH is dripped into the mixture. Mn nanoparticles are also prepared by adding Clove bud extract to a Manganese derivative. For the preparation of nanoparticles, 2ml Manganese acetate was added to 20ml clove extract at 40^0C for 60min. Prepared Mn nanoparticles were stored in a bottle at 4^0C for further characterization.

Measurement techniques

Scanning Electron Microscopy (SEM) was done using Scanning electron microscope FESEM, Model- Quanta 200 FEI to study the morphology of samples; UV-Visible spectroscopy was carried out using UV/Vis spectrophotometer (3092) where the formation of silver nanoparticles was confirmed. Chemical composition was obtained using Fourier Transform Infrared spectroscopy model BRUKER Alpha. Modular Compact Rheometer: Model number MCR 102e was used for Rheological studies like viscosity, storage modulus, and loss modulus. Origin software was used to model the measured data and plot corresponding graph.

Result and Discussion

1. UV-Vis Characterisation

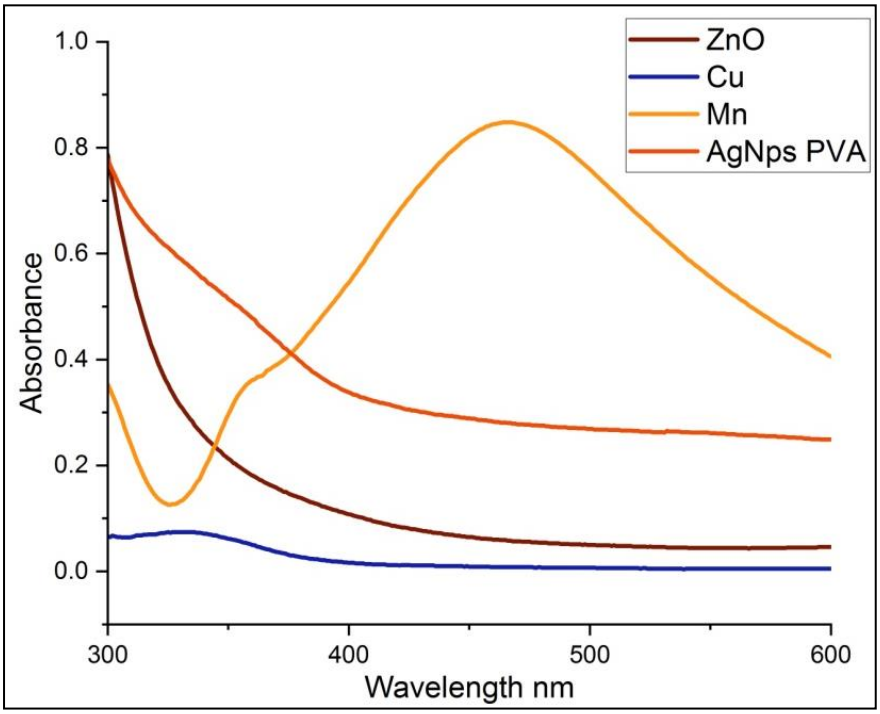

Fig. 1: UV Visible spectroscopy of ZnO, Cu, Mn, and Ag-PVA nanoparticles in the range of 300-600nm

Fig 1 shows the variation in absorption in UV-visible region for ZnO, Cu, Mn, and AgNPs-PVA nanocomposites where, PVA plays the role of a stabilising agent. ZnO nanoparticles when examined immediately after the nanoparticles formation show a very broad curve resembling a peak at the characteristic wavelength of 370nm [11]. Curve of Mn have not shown any particular peak but there is a bump around 360nm which indicates the formation of MnNPs in the sample. This is in compliance with the reports given in the literature for MnNPs [12]. On the other hand, the absorption curve for CuNPs shows minimal absorption hence we didn't find it to be very useful further studies. Moreover, the curve for PVA-AgNps clearly shows the maximum absorption and the characteristic peak at about 459nm confirming the formation of PVA nanocomposites.

2. FTIR

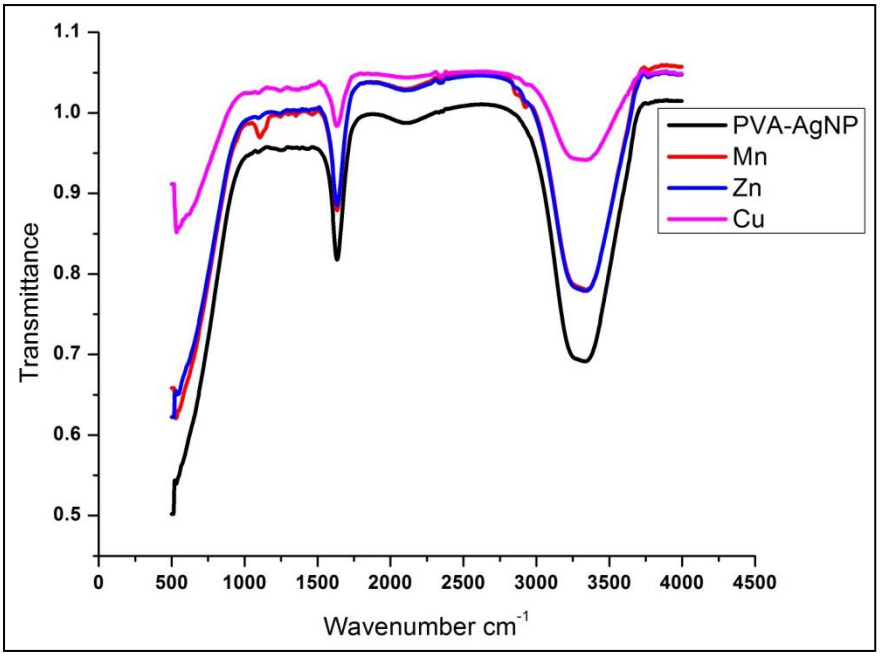

Fig. 2: FTIR spectra of as prepared ZnO, Cu, Mn, and Ag-PVA nanoparticles

Fig 2 shows the FTIR curves obtained for various nanoparticles where the differences in their respective properties were adjudicated. As we can see the curve for Mn-OH bond displays an extra trough for absorption at 1067cm^{-1}[13]. it represents the presence of adsorbed water among the MnO_2 structure. Moreover, the AgNP-PVA demonstrates the highest degree of absorption in the IR region as well. Other than that other nanoparticles do not illustrate any discernable difference in their graphs. Therefore, the Silver nanoparticles with PVA were found to be most responsive here as well.

3. SEM

To investigate the morphological profile of the as-prepared nanoparticles, SEM images were obtained using the FESEM, Model- Quanta 200 FEI. Fig 3 shows the Silver nanoparticles at two different magnifications. It is observable that the nanoparticles have formed small agglomerations along with some nanowires with them as well at around the length of 500nm to 1µm. In Fig 4 the composition of these nanoparticles is observed via EDX analysis where 16.5% of Silver is present.

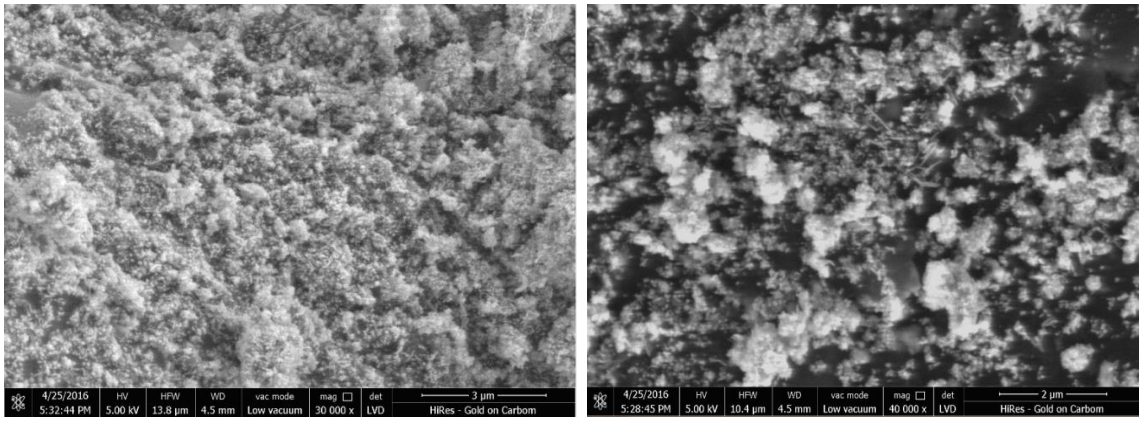

Fig 3: SEM images for AgNPs-PVA nanocomposites

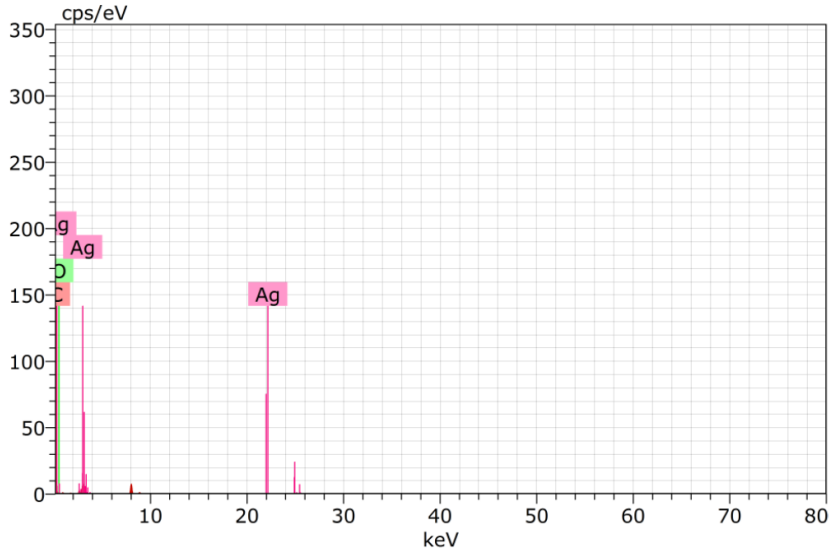

Spectrum: Acquisition 150

El	AN	Series	unn. C [wt.%]	norm. C [wt.%]	Atom. C [at.%]	Error (1 Sigma) [wt.%]
C	6	K-series	82.38	82.38	96.87	2.53
Ag	47	K-series	16.52	16.52	2.16	0.57
O	8	K-series	1.10	1.10	0.97	0.06
		Total:	100.00	100.00	100.00	

Fig.4: EDX results for AgNPs-PVA nanocomposites

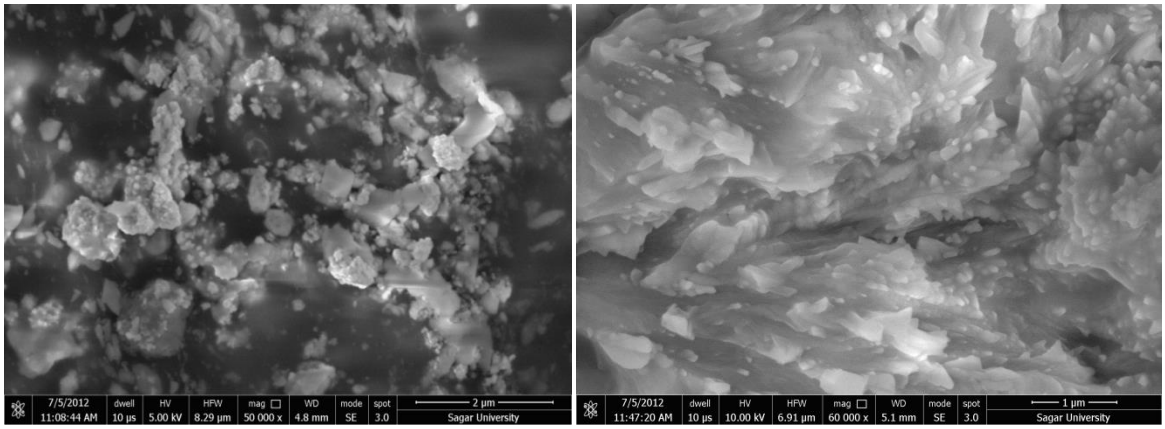

Fig.5: SEM images for Cu NPs prepared using Green synthesis

CuNPs were imaged (fig 5) via SEM where the morphology of nanoparticles are seen to be flaky and the flakes made throughout the sample seem to be homogenous in distribution. Moreover, ZnO nanoparticles were examined at two different resolutions of 2µm and 500nm. Images exhibited the agglomeration of these nanoparticles at about 100nm (fig 6). These conglomerates have been collected to a side hence these nanoparticles are inhomogeneously distributed. Weight percentage of Zn observed using EDX was found to be 75.59% as seen in fig 7.

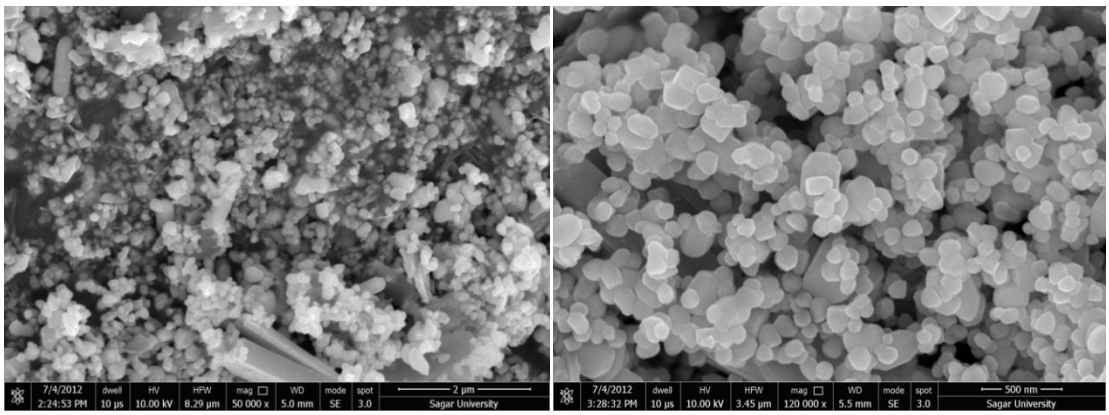

Fig. 6: SEM images for ZnO nanoparticles prepared via Green synthesis

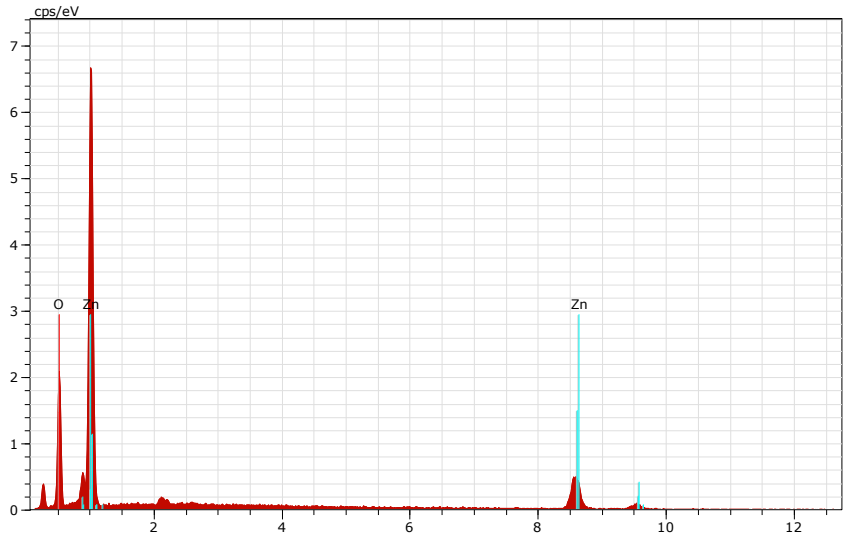

Spectrum: Acquisition

El	AN	Series	unn. C [wt.%]	norm. C [wt.%]	Atom. C [at.%]	Error (1 Sigma) [wt.%]
Zn	30	K-series	53.64	75.79	43.37	2.02
O	8	K-series	17.14	24.21	56.63	2.57
		Total:	70.78	100.00	100.00	

Fig.7: EDX analysis of the ZnO nanoparticles prepared through green synthesis.

SEM images as shown in figure 8 are hexagonal and quite evenly distributed. The aggregation of nanoparticles is a testament to the porous nature of Mn nanoparticles

that may result into the fairly convenient adsorbing properties. The images describe these nanoparticles in as prepared state without any significant impurity in the sample.

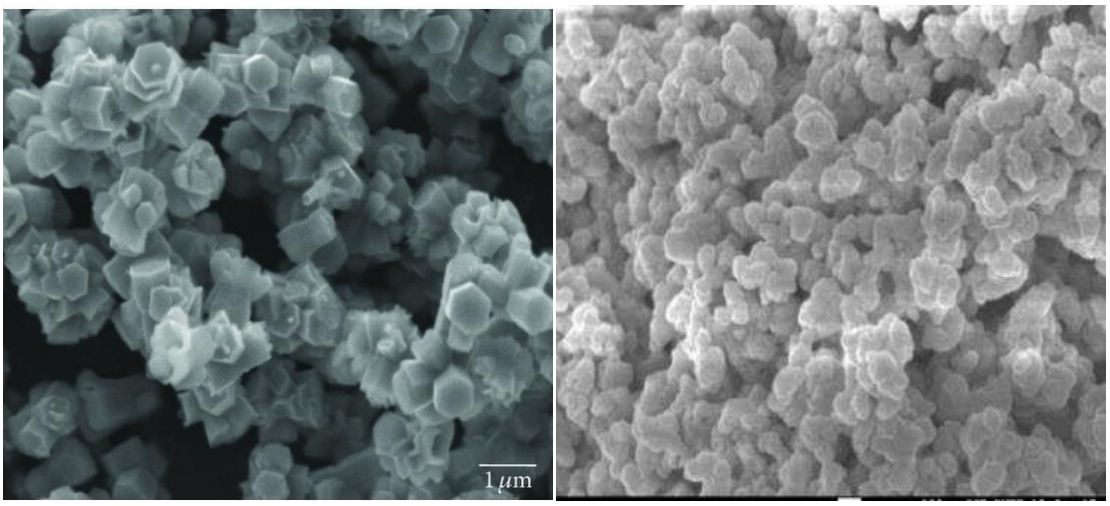

Fig. 8: SEM images for Mn NPs prepared using green synthesis

4. Rheology

Storage modulus, loss modulus, viscosity with time, and Shear strain with frequency of PVA-AgNps gel are given in Fig 9. These results show a solid-like hydrogel behaviour with cross-linked structure. There is a propensity for these values to be higher at lower frequencies and reduce at higher frequencies which may be caused by a decrease in the cross-link density of the PVA gel in the presence of nanoparticles. Similar breaking of cross-link density due to the addition of nanoparticles can also be seen in the reported literature. The decline in the rheological properties of the nanomaterials may be caused by the interaction between the negative electrostatic potential of nanomaterials and polymer chains in PVA [15]. The viscosity of the nanomaterials is given in Fig 9c and it increases with time which may well be explained by the increase in the size of the nanoparticles. Additionally, the decrease in viscosity is given by the agglomeration of particles with increasing frequency.

In Fig 9b storage modulus G' and G'' are displayed as a function of time, the rate of increase of these rheological values with time from 0 to 800s and then beyond 800s these curves take a turn and lower down a little [16]. The reason behind this phenomenon may be the disintegration of Silver nanoparticles at a higher shearing. The gel becomes well dispersed with increasing shearing and hence reduces its luster.

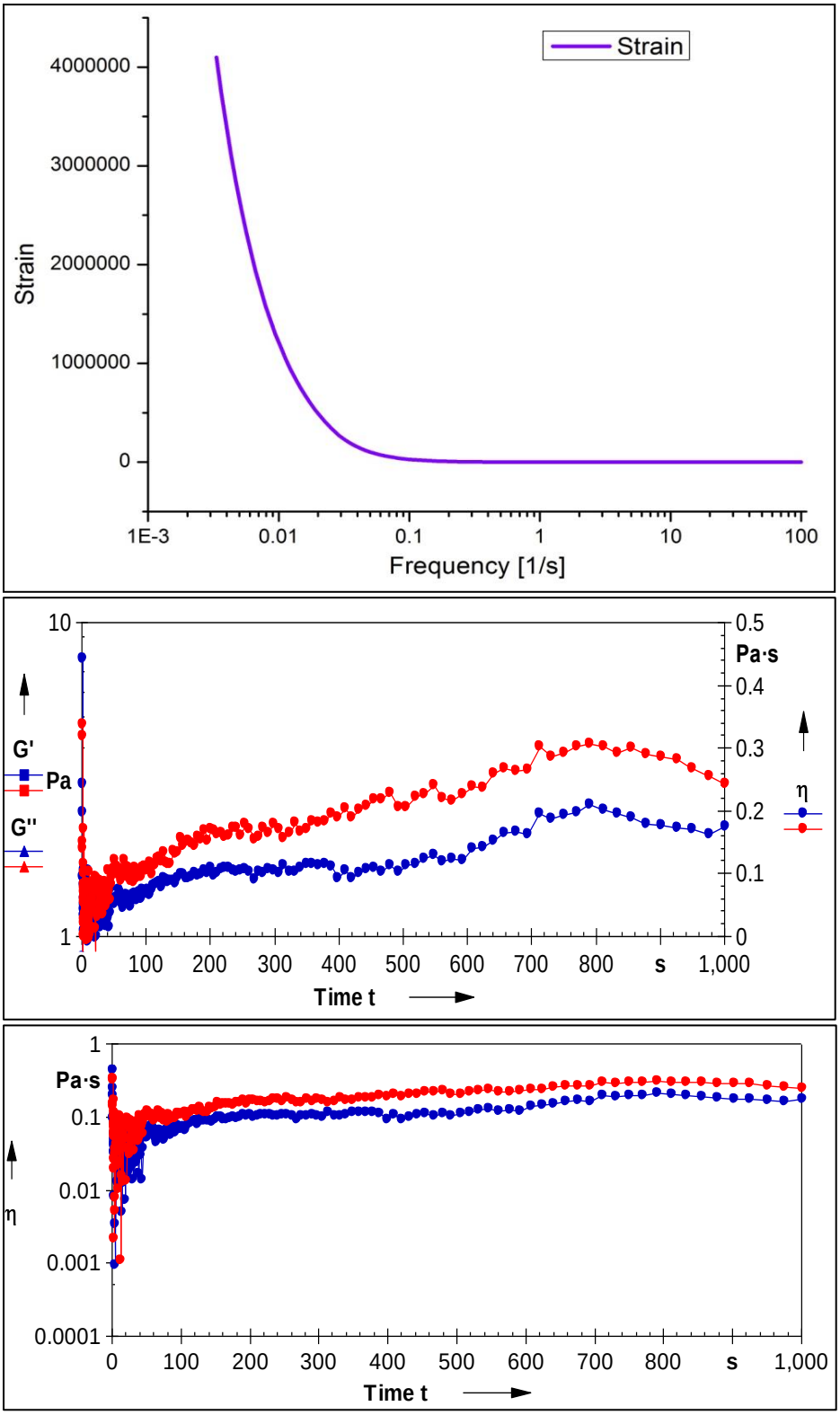

Fig.9: Rheological parameters calculated using the Rheometer a) Shear strain vs frequency graph b) G" and G" vs time graph c) Viscosity (η) vs time graph.

Conclusion

This study discusses the structural properties of nanoparticles made using various metals (AgNPs-PVA, ZnO NPs, MnO_2 NPs, and Cu NPs). Out of these nanoparticles, Silver with PVA gives the best observable properties. UV and FTIR results showed that maximum absorbance was obtained for AgNPs-PVA which meant that these nanocomposites may prove to be most promising to exhibit Rheological properties as well. Absorbance for AgNPs-PVA nanocomposites showed the characteristic peak at 459nm. SEM images showed that all the nanoparticles were synthesized in a well-dispersed manner. EDX studies of Silver nanoparticles and ZnO nanoparticles confirmed the presence of respective elements and the absence of any impurities in the sample. In Rheological studies Silver NPs-PVA nanocomposite gels were found to display non-Newtonian behavior and their viscosity increased with the increase in time of shearing.

References

1. S. A. Khan, S. Patel, P. Shukla, R. Kumar, and R. Dixit, Journal of Scientific Research 66, 139 (2022).
2. N. Bala, S. Saha, M. Chakraborty, M. Maiti, S. Das, R. Basu, and P. Nandy, RSC Advances 5, 4993 (2015).
3. H. Lu, X. Zhang, S. A. Khan, W. Li, and L. Wan, Frontiers in Microbiology 12, (2021).
4. S. C. Mali, A. Dhaka, C. K. Githala, and R. Trivedi, Biotechnology Reports 27, (2020).
5. A. Deutsch, Proceedings of the IEEE 86, 315 (1998).
6. W. Songping, J. Li, N. Jing, Z. Zhenou, and L. Song, Intermetallics 15, 1316 (2007).
7. M. Pospischil, K. Zengerle, J. Specht, G. Birkle, P. Koltay, R. Zengerle, A. Henning, M. Neidert, C. Mohr, F. Clement, and D. Biro, Energy Procedia 8, 449 (2011).
8. R. Alias and S. Mohd, Rheology (2012).
9. S. B. Rane, T. Seth, G. J. Phatak, D. P. Amalnerkar, and M. Ghatpande, Journal of Materials Science: Materials in Electronics 15, 103 (2004).
10. O. Velgosova, L. Mačák, E. Múdra, M. Vojtko, and M. Lisnichuk, Polymers 15, 379 (2023).
11. Shagufta Saeed et al 2021 Mater. Res. Express 8 035004
12. M. Jayandran, M. Haneefa, and V. Balasubramanian, Journal of Applied Pharmaceutical Science 105 (2015).
13. M. Mylarappa, V. V. Lakshmi, K. R. Mahesh, H. P. Nagaswarupa, and N. Raghavendra, IOP Conference Series: Materials Science and Engineering **149**, 012178 (2016).
14. Y. M. Mohan, K. M. Raju, K. Sambasivudu, S. Singh, and B. Sreedhar, Journal of Applied Polymer Science 106, 3375 (2007).
15. Mohan YM, Raju KM, Sambasivudu K, et al.
16. C. Sanchez, D. Renard, P. Robert, C. Schmitt, and J. Lefebvre, Food Hydrocolloids 16, 257 (2002).